DOI: 10.13009/EUCASS2022-6102
9TH EUROPEAN CONFERENCE FOR AERONAUTICS AND SPACE SCIENCES (EUCASS)

Laser Absorption Spectroscopy of Rb at the Longshot Hypersonic Wind Tunnel

DUDÁS Eszter, ANFUSO Enrico*, GROSSIR Guillaume*, CHAZOT Olivier**
** Von Karman Institute for Fluid Dynamics (VKI)*
72 Chaussée de Waterloo 1640 Rhode-St-Genèse Belgium

Abstract
A tunable diode laser absorption spectrometer (TDLAS) is coupled to the world-unique Longshot hypersonic wind tunnel at the von Karman Institute for Fluid Dynamics (VKI) to determine free-stream flow characteristics such as temperature and velocity through non-intrusive measurements. This paper begins with an overview of the theory of the thermal non-equilibrium occurring in hypersonic flow as a possible source of recently reported fluid dynamics anomaly, followed by the presentation of the experimental setup and the preliminary analysis of the first non-intrusive spectroscopic measurement. Finally, following tasks and perspectives are discussed.

1. Introduction

Extensive ground testing of rockets and satellites is essential to ensure sustainable use of the space environment; space hardware past its use-by time must be correctly designed so that it completely demises upon re-entering the Earth atmosphere without posing threats to the ground and without jeopardizing future missions by avoiding residual orbital space debris. [1] The ultimate goal is maintaining clean space, which can be achieved through correct design of space components. In order to properly test spacecraft, the extreme in-flight conditions encountered during re-entry must be recreated on the ground. Hypersonic wind tunnels can briefly reproduce these conditions, yet the fidelity of these ground tests largely relies on the accuracy of their free-stream flow characterisation. Flow quantities in hypersonic wind tunnels must be measured accurately in order to ensure a proper interpretation of the laboratory results, which aim to reproduce the real behaviour of the spacecraft upon re-entry from space. This is a challenging task in high-speed, high-temperature experiments that can typically only be sustained for a few milliseconds each day. Our work aims to develop a novel non-intrusive measurement technique for accurately characterising hypersonic wind tunnel flows using infrared spectroscopy, a novel redundant source of information respect to the existing intrusive probes. This fully independent measurement technique can be used to cross check the existing intrusive methods and will contribute to the improved design of our future satellites in order to maintain a clean space for the next generations.

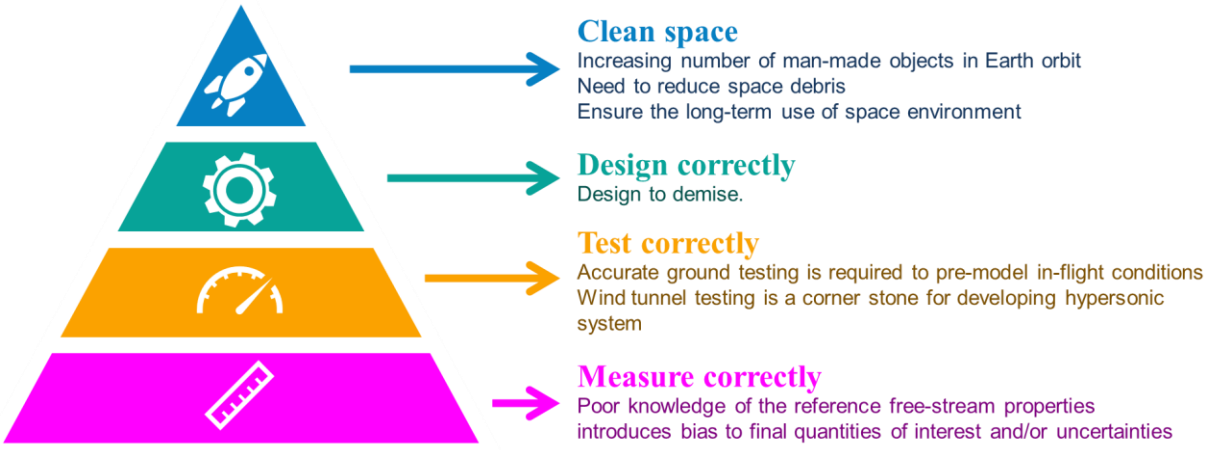

Figure 1: Pyramid of aerospace engineering

DOI: 10.13009/EUCASS2022-6102

Once the mission objectives have been decided and the form of the spacecraft is designed with the aid of numerical simulations, the unit moves to the wind tunnel for testing of its aerodynamics. [2,3] There exists different hypersonic wind tunnel layouts [4] which aim at generating extreme flow velocities. At the von Karman Institute for Fluid Dynamics (VKI), the worldwide unique Longshot facility employs a super-heated gun tunnel to adiabatically compress a large mass of gas before expanding it to hypersonic velocities using specifically designed high-speed nozzles. However, recent flow characterisation test campaigns, relying on intrusive measurement techniques, have uncovered unexpected anomalies later corroborated by additional independent measurements. [5] The observed deviations in the measured pressure values are propagating on derived quantities such as the free-stream Mach number or the Reynolds numbers, which are fundamental similarity parameters for the in-flight conditions. Clearly, the large mismatch highlights the need for an improved understanding of the physics taking place during high-speed flow expansions.
However, improved physical models will only be developed once the underlying physics is fully understood through experiment. The "anomaly" has been observed in different facilities using contoured as well as conical nozzles. [6] Up to date, no definitive explanation has been delivered to explain the discrepancies. A likely explanation, which our project will attempt to demonstrate, is that the hypersonic test gas (N2) is in a state of thermal non-equilibrium. [1] This means that the internal degrees of freedom of the molecules (characterised by rotational, translational, and vibrational modes) do not have the same effective temperature. Hypothetically, a thermal non-equilibrium mechanism could explain a higher free-stream static temperature, since an inefficient vibrational energy relaxation through the hypersonic expansion could result in an out-of-equilibrium state. This has been observed and characterised in studies of high-temperature flows using small-scale nozzles for spectroscopic investigations, [7] and could explain why different measurement techniques provide differing answers. Given the transient nature of facilities such as the Longshot, collecting enough spectral information during a single run is challenging. However, such a feat has been achieved using cavity-enhanced absorption spectroscopy (CEAS) coupled with a shock-tube for the study of chemical kinetics. [8] Our interdisciplinary research project brings together astrophysicist and aerospace engineers to explain hypersonic wind-tunnel flow physics beyond the current level of understanding using established spectroscopic techniques, which have never been applied to this problem before.

2. Non-Local Thermodynamic Equilibrium (non-LTE) state in hypersonic flows

Depending on the medium in which it is located (plasma, supersonic or hypersonic expansion, photosphere, planetary atmosphere, shock layer, etc.), a gas may no longer be in conditions corresponding to a Local Thermodynamic Equilibrium (LTE). LTE is achieved when there are sufficient collisions between the molecules to evenly distribute energy through the different internal degrees of freedom of the molecule, characterised by rotational, translational, and vibrational modes. It usually occurs when the temperature and pressure values are not very low, and the population throughout the quantum energy states follows a Boltzmann distribution and at the same time, the molecular velocity remains Maxwellian. Conversely, when there is a drop in the number of molecular collisions, the abovementioned population distribution differs from a Boltzmann, while the molecular velocity still respects a Maxwellian distribution. This phenomenon is called a non-Local Thermodynamic Equilibrium (non-LTE) [9] and it happens when the radiative lifetimes of certain vibrational energy states are in comparable scale to the mean time between incidents of molecular collisions. [10] In this latter condition, the internal energy populations are not determined strictly by collisional energy exchange and other factors gain importance, such as radiative and chemical pumping as well as radiative losses. [11] The temperature of the gas is inseparably related to the distribution of the molecules throughout their various energy levels, such as rotational, vibrational and electronic energy levels. In case of infrared spectroscopic measurements, electronic states higher than the ground state are generally not activated, therefore the internal energy of the gas is only distributed as translational, rotational and vibrational energies. To precisely describe the partition of the internal energy allocated to rotation or vibration, the characteristic temperature of each has to be determined.

$$T_{vib} = \frac{hcE_{vib}}{kln\left(\frac{g_{vib}n_0}{g_0 n_{vib}}\right)} \quad (1)$$

Here, the notations refer to h - Planck's constant, c - the speed of the light, k - Boltzmann constant, n – the density of molecules and g - the statistical weight of the considered level and E - the energy of the level. The indices *0* refers to the ground state. The same equation can be written for the rotational temperature by substituting the vibrational energy level and statical weight by the rotational ones respectively.

The rovibrational spectroscopic measurements allow to precisely describe how the initial thermal energy of a gas that is stored in the different internal degrees of freedom of the molecule is then redistributed while the gas is expanded to

DOI: 10.13009/EUCASS2022-6102

extreme flow velocities through a nozzle. Previous studies proved that in a hypersonic jet the non-LTE condition is based on a very efficient and quick rotational-translational energy transfer, and a rather inefficient vibrational-translational collisional energy transfer, throughout the adiabatic expansion. [7,12,13] Equation (2) describes what happens to the perfect gas energy wise through an adiabatic expansion.

$$c_p T_o = c_p T + \frac{1}{2} v^2 \quad (2)$$

Where c_p - is the heat capacity at constant pressure, T_o and T are the initial and static temperatures respectively, and v is the local flow speed. The left hand side of the equation represents the total initial energy that has been communicated to the system meanwhile the right side describes the partition of it as it is converted into kinetical and thermal energies. To be noted that in case of the Longshot facility due to high-stagnation temperatures calorically imperfect behavior is needed to be taken into account.

At the same time, the Mach number, a dimensionless variable defined by the ratio of the local flow speed (v) to the local sound speed (a):

$$Ma = \frac{v}{a} \quad (3)$$

can be considered as a ratio between the kinetic energy characterizable by the velocity (v) of the gas and the thermal energy of the gas (as the sound speed (a) depends on temperature). Thus, a flow accelerating adiabatically may reach extremely low temperatures associated with very high Mach numbers ($T \rightarrow 0$K, $M \rightarrow \infty$).

$$Ma = \frac{v}{\sqrt{\gamma r T}} \propto \sqrt{\frac{E_{kinetic}}{E_{thermal}}} \quad (4)$$

where r stands for the universal gas constant (R) weighted by the molar mass ($\mathcal{M}$) of the atom/molecule ($r = R/\mathcal{M}$) and γ is the specific heat ratio.

In case of an LTE state the temperature value in the above mentioned equation can be described with one characteristic value, however once the gas is in a non-LTE state distinction must be made between translational, rotational and vibrational temperatures. Such a state could be the culprit of the reported anomaly [5] and would explain the achieved lower Ma number at the Longshot facility as well as.

3. Experimental setup

3.1 VKI Longshot hypersonic tunnel

The VKI Longshot hypersonic tunnel (see figure (2)) serves as a unique facility for ground testing measurements at high Mach numbers and at relatively large Reynolds numbers, in a near-perfect gas environment free from chemistry effects. It is currently established as a reference wind tunnel for investigating Earth re-entry trajectories in a low - enthalpy environment. [14–17]

DOI: 10.13009/EUCASS2022-6102

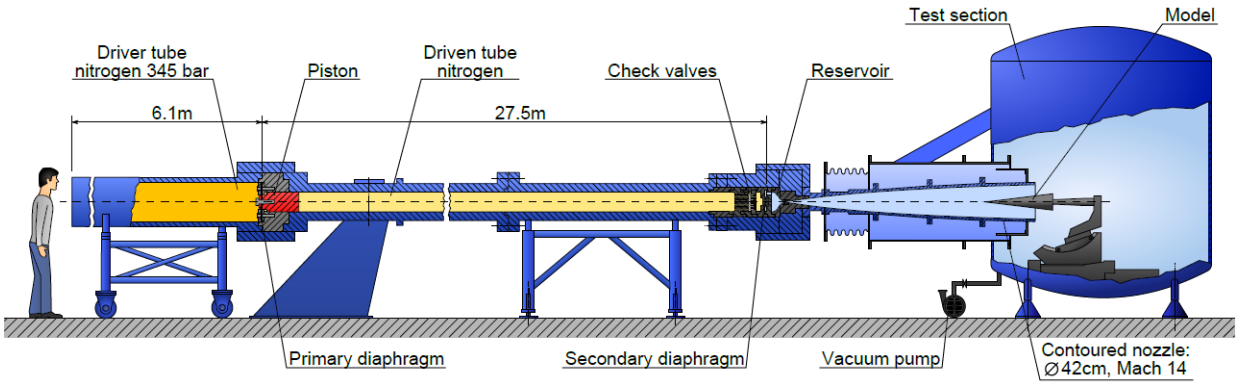

Figure 2: Sketch of the VKI Longshot hypersonic gun tunnel [18]

The facility operates on the gun tunnel principle and usually uses pure nitrogen as a test gas. During operation, an inertial piston compresses the test gas up to stagnation pressure and temperature, around 400 MPa and 2500 K respectively. Conveniently, the total enthalpies remain sufficiently low to prevent chemical reactions of nitrogen from occurring. The test gas is then expanded within one of the hypersonic nozzles currently available (two contoured nozzles for Mach 12 and Mach 14, one conical nozzle within the range Mach 10-20) for test durations on the order of 10-20 ms.
VKI conducted systematic investigations for flow characterisation and a dedicated state-of-the-art methodology has been implemented in order to derive all free-stream flow quantities of interest based on the few measurements available (pitot pressure, free-stream static pressure, and stagnation point heat flux measurements). [5] The methodology relies on the VKI Mutation++ library [19] which accounts for transport and thermodynamic properties of the test gases at high temperatures. [18,20] The characterisation of the Longshot flow expansions is subject to stringent constraints that raise several challenges from spectroscopic point of view. One of the biggest constraints arises from the short (less than 20 ms) test time further stressed by a low (one run per day) duty cycle. During the run itself, additional transients have to be considered, as the flow gradually slows down. Potential issues associated with mechanical vibrations will also need to be anticipated. The goal is therefore to carefully design experiments accounting for all these constraints to ensure the success of the investigations.

3.2 Tunable diode laser absorption spectrometer

A laser beam passing through a layer of homogenous gas loses a certain quantity of its initial intensity ($I_0(\nu)$) at a given wavenumber (ν). The absorption feature of the gaseous medium can be described by the Beer-Lambert law [21]:

$$I(\nu) = I_0(\nu) * \exp\left(-\alpha(\nu, [T, n]) * l\right) \quad 5$$

Where, $\alpha(\nu)$ - spectral absorption coefficient in cm^{-1}, T and n are the temperature and density of the gas; and l - the pathlength of the studied layer of gas. By defining the integrated absorption coefficient (σ) of an isolated line centred at ν_0:

$$\sigma = \int_{-\infty}^{\infty} \alpha(\nu - \nu_0) d(\nu - \nu_0) \quad 6$$

the spectral absorption coefficient can be determined using the integrated absorption coefficient as a proportionality constant and a normalized profile ($\Phi(\nu - \nu_0)$) whose integral over the entire spectral domain is unity:

$$\alpha(\nu - \nu_0) = \sigma\Phi(\nu - \nu_0) \quad 7$$

This $\Phi(\nu - \nu_0)$ profile, or shape function is the key to investigate the different flow characteristics, as the occurring broadening and shifting of this profile will reveal the temperature and the velocity of our gas in the core flow. In this study we will use the thermal Doppler line broadening to determinate the translational temperature of our gas, as the broadening results in Gaussian profile which can be characterised with the temperature dependent full width at half maximum (FWHM) of the atom:

DOI: 10.13009/EUCASS2022-6102

$$FWHM = \frac{2\sqrt{2Rln(2)}}{c}\nu_0\frac{T_{tr}}{M} \quad 8$$

Where, R – is the universal gas constant, c – is the speed of light and M – represents the molar mass. However, it is to be remembered that the determined translational temperature is only linked to the kinetic energy of the gas and in case of a non-LTE condition the above obtained temperature does not reveal any information of the thermal energy of the gas. Panel (a) of figure (3) demonstrates the temperature dependence of a spectral line shape, and highlights the different characteristic FWHM at various temperature values.

On the other hand, to estimate the velocity of the hypersonic jet, the shift of the line position over the spectral domain is investigated as the Doppler effect describe a relative velocity between the atom moving with the jet and the laser beam. The frequency shift of the recorded line solely depends on the velocity (u) of the atom and the angle (θ) between this velocity vector and the laser beam.

$$\nu_{shift} = \nu_0\frac{u}{c}\cos(\theta) \quad 9$$

Panel (a) of figure (3) represent the shift occurring at various flow velocity conditions. In our system, the angle is $\theta = 11.2°$ which suggests a typical Doppler shift $\nu_{shift} = 0.04\ cm^{-1}$ for a flow velocity of u = 1000 m.s^{-1}. As we have a single pass through the gaseous medium, the direction of the shift depends on the direction of the laser beam.

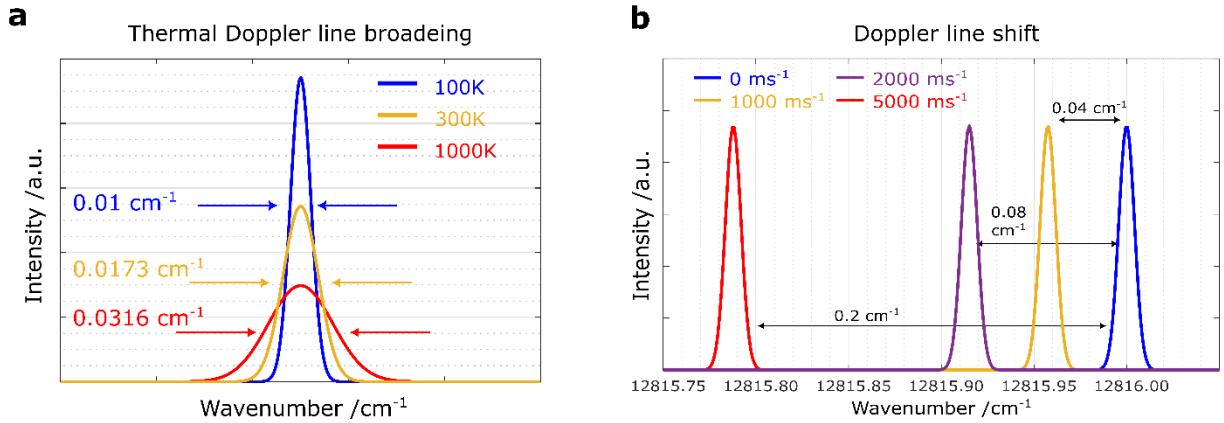

Figure 3: panel (a): represents the temperature dependence of the thermal Doppler line broadening. Panel (b) highlights the concept of the Doppler shift at various flow velocities

To carry out spectroscopic measurements, a tracer gas must be admixed to the otherwise pure nitrogen flow, which itself is not spectroscopically detectable in the infrared. Following the successful measurements in the High Enthalpy Shock Tunnel HEG of the German Aerospace Center (DLR) rubidium (Rb) has been selected as a seeded species. It is an advantageous choice as its spectroscopic features have been widely studied before [22–25]. Natural rubidium consists of two isotopes ^{85}Rb and ^{87}Rb representing 72% and 28% of relative proportion respectively. Figure (4) represents the energy structure of the rubidium highlighting the transitions from its ground state ($^2S_{1/2}$) to its higher state configuration ($^2P_{3/2}$) state, occurring around 780 nm. The hyperfine states are characterised by quantum number F which represents the interaction of the nuclear magnetic moment and the internal field of the rubidium atom. The selection rule for dipole transitions allows $\Delta F = 0, \pm 1$; and taken into account that the energy differences are orders of magnitude higher between the two $^2S_{1/2}$ hyperfine levels compared to the differences between the $^2P_{3/2}$ hyperfine levels the transitions for each isotopes regroups into two packages of three lines. In our case we will consider the transitions starting $F_g = 2 \rightarrow F_e = 1,2,3$ for the isotope ^{87}Rb and $F_g = 3 \rightarrow F_e = 2,3,4$ for isotope ^{85}Rb.

DOI: 10.13009/EUCASS2022-6102

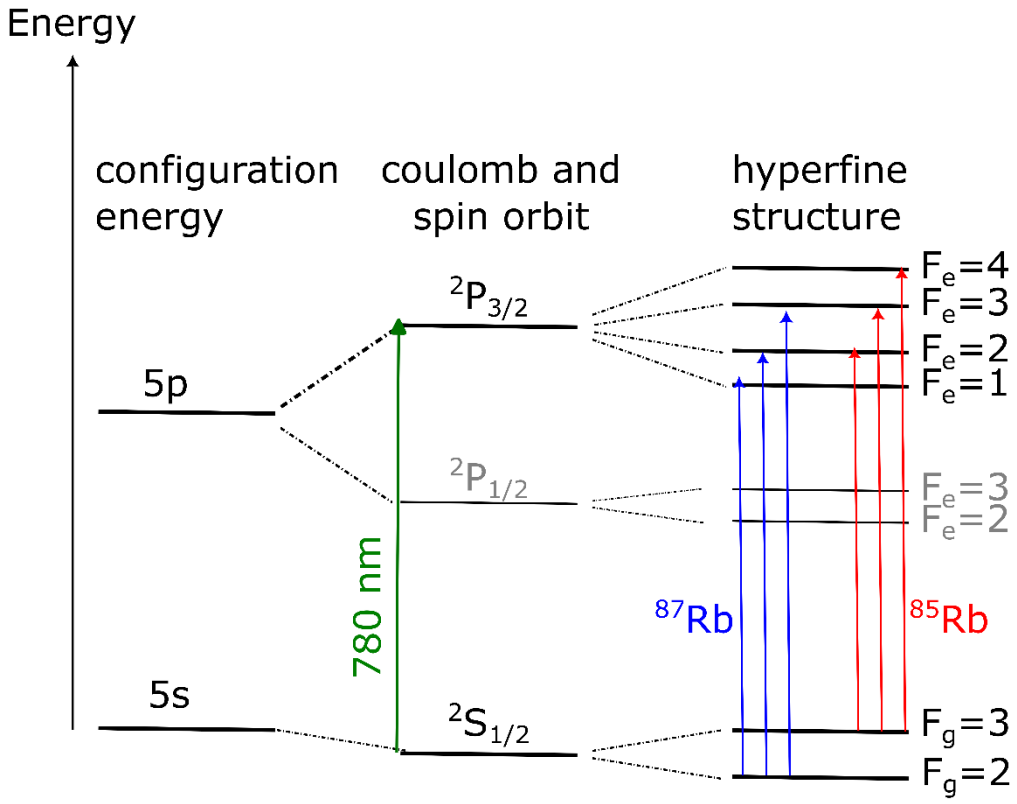

Figure 4: Hyperfine energy structure of the two natural isotopes of Rb

Carrying out spectroscopic measurements in the Longshot facility means overcome a series of challenges. The experimental setup is presented in figure (5), the test chamber is directly connected to the gun tunnel and therefore, with the arrival of the jet, massive vibration takes place. In order to avoid adding noise to the optical system, it is all constructed around the test chamber on separate tables. However, it means that the laser beam has to run a longer path, containing ambient air and wide windows on the test chamber wall. This latter ones additionally slightly move once the flow arrives to the chamber and the pressure starts increasing. A single mode TOPTICA® Distributed-feedback (DFB) pro laser emits at ~780 nm and to achieve multiple scans in the available short test time (10-20 ms) the laser head is directly modulated via Mod DC connectors at 500 Hz, up to 11mA. These modulations are applied as offsets to the diode current set from the laser driver controller and aren't limited by the controller electronics and they could go up to 100MHz and it requires the use of an external function. To determine the Doppler shift an etalon signal is used and therefore, the initial laser beam is split into two equal parts by a 50-50 beam splitter. One part goes directly into the test chamber through the window access, meanwhile the second half of it passes through a rubidium vapor reference cell. In this cell the gas is in steady state with zero flow velocity, and as equation (9) describes there is no Doppler shift occurring. As the laser beam probes the flow along a line of slight, unwanted boundary layer contribution could appear into the integrated absorption spectrum. However, previous study [26] has proven that two shear layer shields, closely positioned downstream of the nozzle exit could skim the shear layer of the flow and therefore reduce the hot gas contribution. The rubidium is admixed to the flow up-steam of the nozzle throat. Knowing that the Rb is a reactive alkali metal in ambient conditions, it cannot directly be seeded to the flow. Instead of it, rubidium nitrate ($RbNO_3$), whose molecular weight is 147.47 $g.mol^{-1}$, is priorly admixed with water and the mixture is painted onto the secondary diaphragm prior to the reservoir and onto the convergent part of the nozzle. With the arrival of the shock on the diaphragm, the $RbNO_3$ decomposes and melts and atomic Rb blends into the N_2 flow. Additionally to the TDLAS setup, intrusive probes such as stagnation heat flux probes, stagnation point pressure probe and static pressure probe are installed to rebuild the free-stream flow properties.

DOI: 10.13009/EUCASS2022-6102

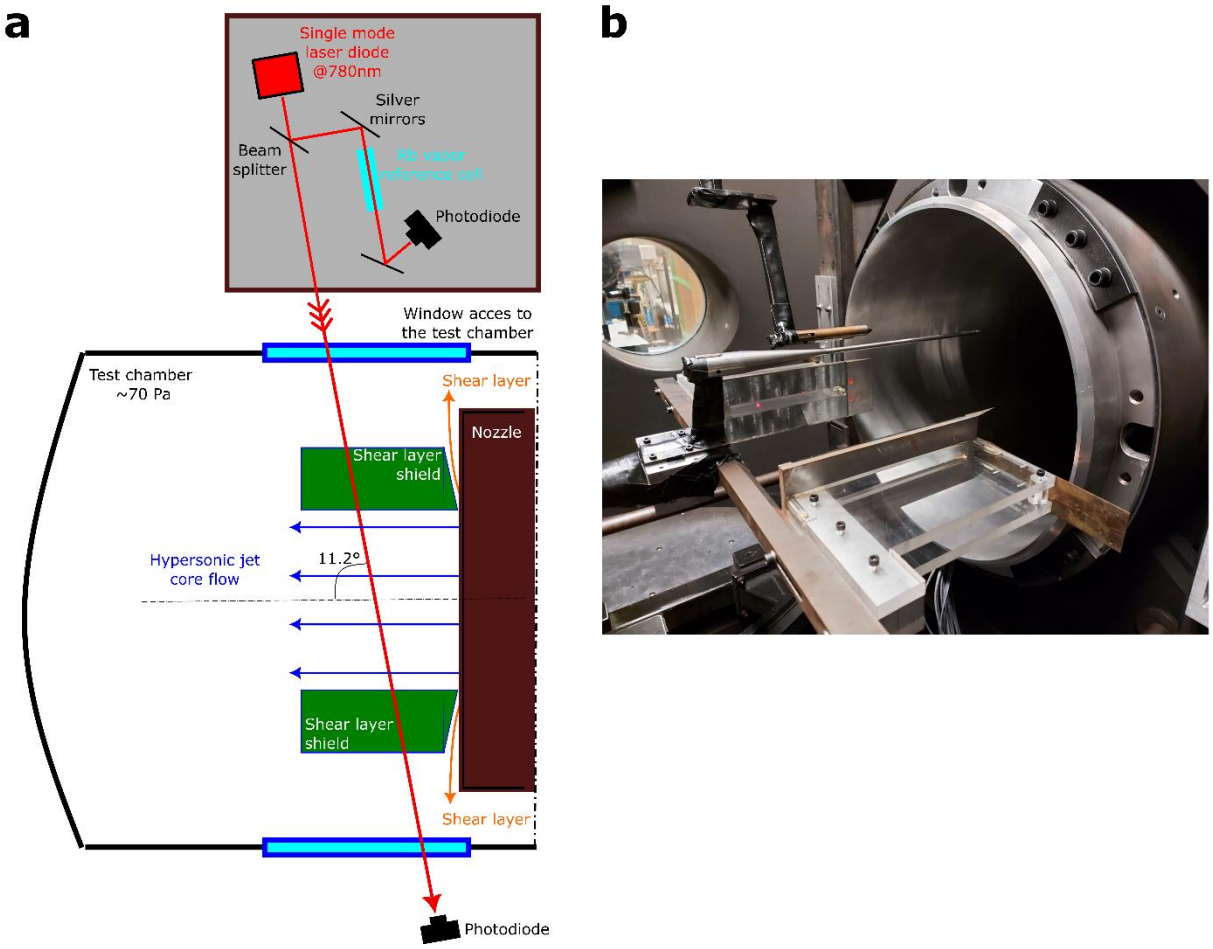

Figure 5: Experimental setup. Panel (a) is a schematic representation of the TDLAS coupled to the Longshot facility. Panel (b) is a photo of the inside of the test chamber highlighting the shear layer shields and the intrusive probes.

4. Preliminary results

Only two test runs have been conducted up to date in the Longshot facility with the TDLAS setup. In test run 1866, Rb lines from the core flow did not appear in the spectra, only the recirculating, low velocity, hot gas contribution was detected starting from 7 ms after the arrival of the jet. For the next run, the concentration of the $RbNO_3$ has been increased to seed more rubidium into the flow and although, it is essential to underline this is only a preliminary analysis of the first results, in test run 1867: cold and high velocity Rb contribution is believed to be detected in the spectrum. Figure (6) panel a presents the evaluation of the stagnation point pressure, during the red zone the flow is the hypersonic nozzle flow is being established, however from 4 ms until a little bit more than 15 ms a cold uniform core flow is present. Underneath, in panel b the recorded etalon spectra (red) and the recorded jet spectra (blue) is plotted. Probably due to heavy vibration and turbulent flow behaviour, the recorded data is very noisy in the instable region, however once the uniform flow is established the signal quality improves.

DOI: 10.13009/EUCASS2022-6102

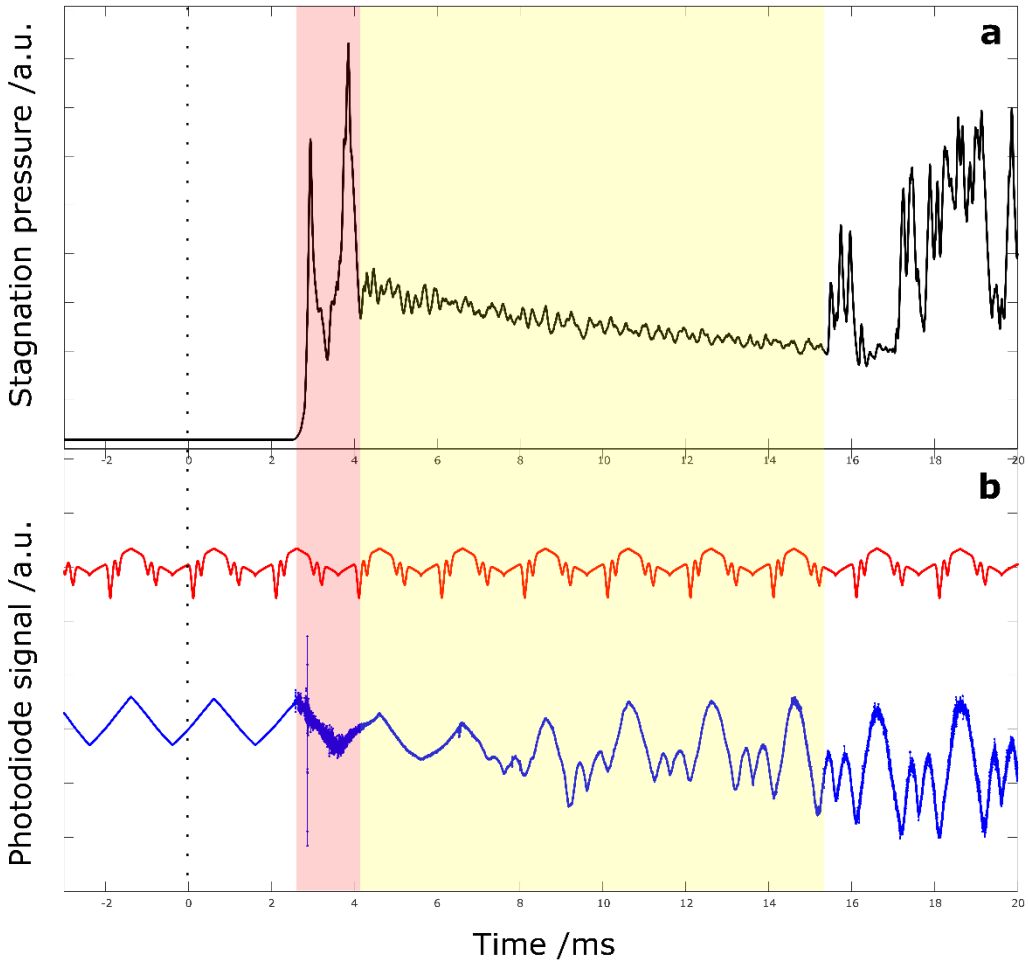

Figure 6: experimental results, red domain represents the arrival of the jet meanwhile the yellow domain corresponds to the presence of the uniform core flow. Panel (a) displays the stagnation pressure measured in the core flow. Panel (b) shows the etalon photodiode signal (red) and the jet photodiode signal (blue).

The first signal of cold and Doppler shifted rubidium lines appear on the scan around 6 ms. Unfortunately from 7 ms the recirculating gas with its hot gas contribution arrives into the laser beam path. Nevertheless, a preliminary flow velocity was calculated from the occurring Doppler shift, resulting in a $u = 2195$ m.s^{-1}. Figure (7) highlights the theoretical line positions for the two isotopes of the rubidium, as well as the baseline corrected and frequency domain converted etalon signal and jet signal and lastly the jet signal with the Doppler shift offset. Looking into the thermal Doppler broadening of the lines, a FWHM = 0.0094 cm^{-1} was measured by fitting a Gaussian profile over the absorption line profiles and this corresponds to a translational temperature $T_{trans} = 89(40)$ K. As a next step, this velocity and temperature value will be compared to the flow velocity and temperature obtained from the flow rebuild process.

DOI: 10.13009/EUCASS2022-6102

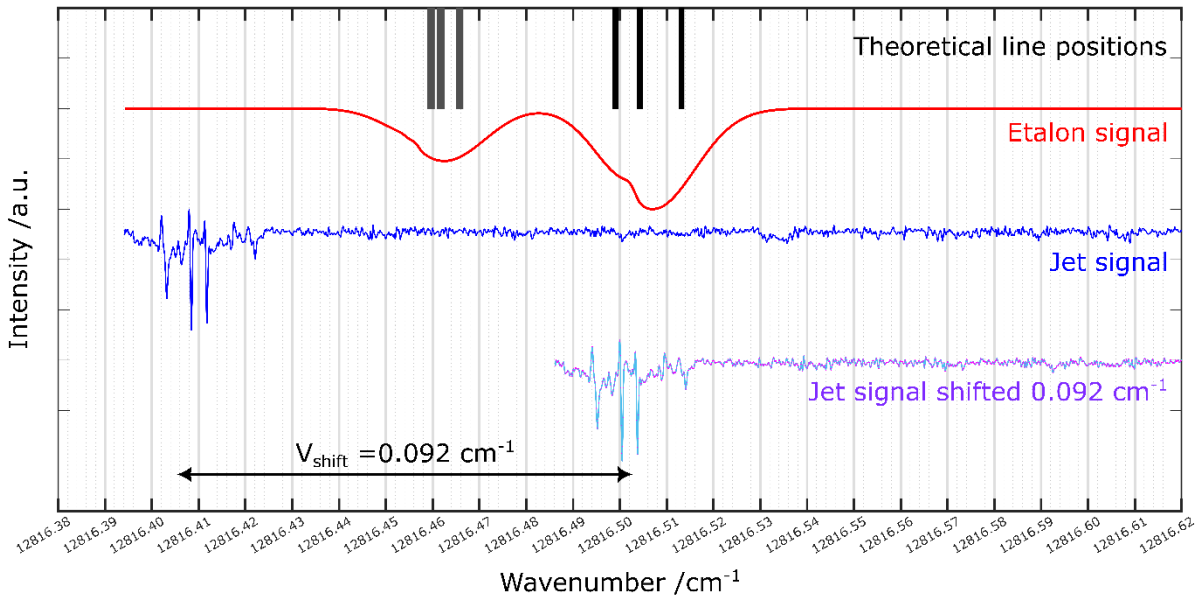

5. Discussion and perspectives

As previously has been mentioned, only two test have been conducted yet, therefore following tests should confirm if the preliminary analysis is correct. Nevertheless, for the upcoming runs, a more precisely controlled Rb seeding process should be adopted to ensure the comparability of the test results as well as to ensure that sufficient Rb is admixed into the flow. To avoid the unwanted contribution of the recirculating hot gas, the laser beam path should be protected up to the shear layer shield, therefore the design of a protection obstacle is in progress.

Looking further into the project, in order to examine the energy distribution into different internal degrees of freedom of the molecule, absorption peaks issuing from different vibrational and rotational levels must be simultaneously recorded. Therefore, a different tracer gas will be introduced to the system. Carbon monoxide is a suitable choice, since it has a similar molecular weight, specific heat capacity, standard entropy, polarizability and same internal degrees of freedom as nitrogen. All these characteristics result in its fluid behaviour being sufficiently similar to that of nitrogen to permit its direct substitution without significantly altering the nozzle flow expansion. At the same time, the choice of the probe molecule is based on the fact that CO is a very well-studied molecule exhibiting a simple infrared spectrum, the line positions of both its cold bands and hot bands are precisely referenced in databases such as HITRAN. [27] The relative spectra produced from these three different diodes will enable the determination of the free-stream vibrational and rotational temperature as well.

6. Acknowledgments

Mikel Spillemaekers is acknowledged for his continuous assistance and support in operating the Longshot facility. This material is based upon work supported by the Air Force Office of Scientific Research under award number FA8655-20-1-7024.

DOI: 10.13009/EUCASS2022-6102

References

[1] Grossir G, Puorto D, Ilich Z, Paris S, Chazot O, Rumeau S, et al. Aerodynamic characterization of space debris in the VKI Longshot hypersonic tunnel using a free-flight measurement technique. Exp Fluids 2020;61:163. https://doi.org/10.1007/s00348-020-02995-7.

[2] Carbonaro M. Aerodynamic Force Measurements in the VKI Longshot Hypersonic Facility. In: Boutier A, editor. New Trends in Instrumentation for Hypersonic Research, Dordrecht: Springer Netherlands; 1993, p. 317–25. https://doi.org/10.1007/978-94-011-1828-6_29.

[3] Beck J, Caiazzo A, Gülhan A, Innocenti L, Schleutker T, Soares T. Plasma Wind Tunnel Demisability Testing of Spacecraft Equipment, 2019, p. 10.

[4] Lu F, Arnold DM. Advanced Hypersonic Test Facilities. Illustrated edition. Reston, Va: AIAA; 2002.

[5] Grossir G, Van Hove B, Paris S, Rambaud P, Chazot O. Free-stream static pressure measurements in the Longshot hypersonic wind tunnel and sensitivity analysis. Exp Fluids 2016;57:64. https://doi.org/10.1007/s00348-016-2137-5.

[6] William J. Etude des processus physico-chimiques dans les écoulements détendus à haute enthalpie : application à la soufflerie à arc F4. Université de Provence. Section sciences, 1999.

[7] Dudás E, Suas-David N, Brahmachary S, Kulkarni V, Benidar A, Kassi S, et al. High-temperature hypersonic Laval nozzle for non-LTE cavity ringdown spectroscopy. J Chem Phys 2020;152:134201. https://doi.org/10.1063/5.0003886.

[8] Sun K, Wang S, Sur R, Chao X, Jeffries JB, Hanson RK. Sensitive and rapid laser diagnostic for shock tube kinetics studies using cavity-enhanced absorption spectroscopy. Opt Express 2014;22:9291. https://doi.org/10.1364/OE.22.009291.

[9] Gamache RR, Vispoel B, Rey M, Tyuterev V, Barbe A, Nikitin A, et al. Partition sums for non-local thermodynamic equilibrium conditions for nine molecules of importance in planetary atmospheres. Icarus 2022:114947. https://doi.org/10.1016/j.icarus.2022.114947.

[10] Edwards DP, López-Puertas M, Gamache RR. The non-LTE correction to the vibrational component of the internal partition sum for atmospheric calculations. Journal of Quantitative Spectroscopy and Radiative Transfer 1998;59:423–36. https://doi.org/10.1016/S0022-4073(97)00125-8.

[11] Herzberg G. Infrared and Raman spectra of polyatomic molecules. New York: Van Nostrand; 1945.

[12] Louviot M, Suas-David N, Boudon V, Georges R, Rey M, Kassi S. Strong thermal nonequilibrium in hypersonic CO and CH4 probed by CRDS. J Chem Phys 2015;142:214305. https://doi.org/10.1063/1.4921893.

[13] Suas-David N, Kulkarni V, Benidar A, Kassi S, Georges R. Line shape in a free-jet hypersonic expansion investigated by cavity ring-down spectroscopy and computational fluid dynamics. Chemical Physics Letters 2016;659:209–15. https://doi.org/10.1016/j.cplett.2016.06.082.

[14] Perry R. The Longshot type of high-Reynolds number hypersonic tunnel. Advanced experimental techniques for study of hypervelocity ight, 1964.

[15] Richards BE, Enkenhus KR. Hypersonic testing in the VKI longshot free- piston tunnel. AIAA Journal 1970;8:1020–5. https://doi.org/10.2514/3.5825.

[16] Simeonides G. The performance of the VKI longshot hypersonic wind tunnel 1987.

[17] Grossir G, Pinna F, Chazot O. Influence of Nose-Tip Bluntness on Conical Boundary-Layer Instabilities at Mach 10. AIAA Journal 2019;57:3859–73. https://doi.org/10.2514/1.J057822.

[18] Grossir G. Longshot Hypersonic Wind Tunnel Flow Characterization and Boundary Layer Stability Investigations. 2015. https://doi.org/10.13140/RG.2.1.2394.0720.

[19] Magin TE. A model for inductive plasma wind tunnels. Université libre de Bruxelles, n.d.

[20] Grossir G, Dias B. Flow characterization of the VKI Longshot wind tunnel. Flow characterization and modeling of hypersonic wind tunnels, vol. VKI Lecture Series 2018/19, chapter 3, 2018.

[21] Penner SS. Quantitative molecular spectroscopy and gas emissivities. Reading, Mass.: Addison-Wesley Pub. Co.; 1959.

[22] Beck WH. Spectroscopic Techniques for Measurement of Velocity and Temperature in the DLR High Enthalpy Shock Tunnel HEG. DEUTSCHES ZENTRUM FUR LUFT-UND RAUMFAHRT EV GOETTINGEN (GERMANY) INST FOR FLUID MECHANICS; 2000.

[23] Krmpot AJ, Rabasović MD, Jelenković BM. Optical pumping spectroscopy of Rb vapour with co-propagating laser beams: line identification by a simple theoretical model. J Phys B: At Mol Opt Phys 2010;43:135402. https://doi.org/10.1088/0953-4075/43/13/135402.

[24] Ben-Aroya I, Eisenstein G. Characterizing Absorption Spectrum of Natural Rubidium by Using a Directly Modulated VCSEL, 2005, p. 602–7.

[25] Barwood GP, Gill P, Rowley WRC. Frequency measurements on optically narrowed Rb-stabilised laser diodes at 780 nm and 795 nm. Appl Phys B 1991;53:142–7. https://doi.org/10.1007/BF00330229.

DOI: 10.13009/EUCASS2022-6102

[26] Meyers J. Tunable Diode Laser Absorption Spectroscopy Characterization of Impulse Hypervelocity CO2 Flows. Universit e Libre de Bruxelles, 2009.
[27] Gordon IE, Rothman LS, Hill C, Kochanov RV, Tan Y, Bernath PF, et al. The HITRAN2016 molecular spectroscopic database. Journal of Quantitative Spectroscopy and Radiative Transfer 2017;203:3–69. https://doi.org/10.1016/j.jqsrt.2017.06.038.